



## ORIGINAL ARTICLE

# Geodetic monitoring of earth-filled flood embankment subjected to variable loads

Przemysław Kuras<sup>1\*</sup>, Łukasz Ortyl<sup>1</sup>, Tomasz Owerko<sup>1</sup> and Aleksandra Borecka<sup>2</sup>

<sup>1</sup>Department of Engineering Surveying and Civil Engineering, Faculty of Mining Surveying and Environmental Engineering, AGH University of Science and Technology, 30 Mickiewicza Av., 30-059, Cracow, Poland

<sup>2</sup>Department of Hydrogeology and Engineering Geology, Faculty of Geology, Geophysics and Environmental Protection, AGH University of Science and Technology, 30 Mickiewicza Av., 30-059, Cracow, Poland

\*kuras@agh.edu.pl

## Abstract

The article presents an example of supplementing geotechnical monitoring with geodetic observations. The experimental flood embankment built within the ISMOP project (Information Technology System of Levee Monitoring) was subjected to continuous monitoring based on built-in measuring sensors. The results of geodetic monitoring used for observation of earth-filled flood embankment subjected to external loads are presented in the paper.

The tests were carried out on an experimental flood embankment forming a closed artificial water reservoir.

The observations were carried out for two purposes. The first was long-term monitoring, which was aimed to determine the behaviour of the newly built embankment. The second purpose was to check the reaction of the levee to the simulated flood wave, caused by filling and draining the reservoir.

In order to monitor the displacements of the earth-filled embankment, it was necessary to develop the proper methodology. For the needs of research works, an appropriate network of 5 reference points and 48 survey markers has been designed and established. The periodic measurements were carried out using precise robotic total station. The stability of the reference frame was each time checked and displacements of survey markers were determined based on it.

The final results allow to reveal the reaction of levee to external loads. The displacement values were referred to the course of the filling and draining experiment to indicate the relationship between them. In the field of long-term monitoring the results clearly imply the dominance of displacements outside the reservoir for points located on the embankment, in contrast to points on the crest and foreground, which do not show significant movements. On the other hand, in the field of testing the embankment reaction to the flood wave, obtaining reliable results was possible thanks to high-accuracy geodetic measurements. Small displacement values, often at the level of their determination errors, were averaged for groups of points with the same height of foundation. A sizable number of points allows to perceive some tendencies and the relation between embankment soaking, hence its movement directions can be noticed. During periods when the levee was still saturated with water, slight movements outside the reservoir were revealed. On the other hand, the following period of drying caused movement in the opposite direction.

**Key words:** flood embankment, river levee, geodetic monitoring, control network, displacements

## 1 Introduction

### 1.1 Motivation for experimental embankment construction

Flood protection is an important component of a comprehensive approach to crisis management. One of the forms of passive flood protection are flood embankments. It is a type of damming structure whose task is to limit the extent of flooding riverside areas by the water of the flooded river, rather than eliminate it. Flood embankments take on the function of damming structure only during the freshets. If the time of high water levels is long enough, a filtration regime in the embankment body is shaped similar to that observed in the body of the earth-filled dam with constant damming.

The problem of flooding was, is and will be a serious threat in Poland, mainly due to the poor condition of flood protection systems. Early detection and precise determination of the leakage place and dynamics of the destructive process development are crucial for minimizing the risk of failure or its range by making early and optimal decisions resulting in effective preventive or repair activities while minimizing their costs. Efficient management and the use of innovative solutions in flood monitoring affect the effectiveness of actions of the authorities and administration at all levels, as well as the competence of other social and economic entities responsible for crisis management during the flood (Borecka, 2016).

A conscious state policy in the field of prevention and minimization of losses is becoming an indispensable and even superior task of flood protection. This can be implemented through appropriate management of the area threatened by flooding, raising public awareness of flood hazards and teaching how to live with floods, and creating monitoring and early warning systems (Filaber et al., 2016).

In order to investigate the phenomena occurring in the flood embankments the IT System of Levee Monitoring (ISMOP) was created. A system approach to the issue of flood earth embankment monitoring is the aim of the project. The purpose of the research is the creation of a system which monitors the static and dynamic behaviour of levee in real time. ISMOP is aimed at the mass gathering of data concerning selected processes taking place in the levee, optimization of data transfer as well as the interpretation and analysis, with the use of numerical simulations, and a system of visualization of the levee's condition (Stanisz et al., 2015).

Deformation of the levee results from the hydraulic pressure of water, water filtering through the levee and its subsoil, and the hydrating and drying of the levee material. This process is intensified under the influence of an increased level of water during a flood. Under conditions of change in water pressure, the development of the deformation process often leads to the failure of the levee (Stanisz et al., 2017).

### 1.2 State of the art of horizontal displacement determination

Geotechnical monitoring allows to determine changes taking place in a structure as well as their sources and mutual dependencies. Geotechnical key parameters (such as inclination, stress or temperature) are usually measured using various types of sensors. However, geodetic methods are irreplaceable to determine the location of a measuring point (and also its changes). According to the International Organization for Standardization (ISO, 2015), "for the support, evaluation, and control of geotechnical measurements, reference shall be made to geodetic measurements if applicable". The effects resulting from the mutual complementation of geotechnical monitoring

and geodetic observations are presented by Hwang et al. (2008) on the example of ground studies for high speed rail, or Ghorbani et al. (2012) to identify tunnelling hazards in urban areas.

Among the series of measurements aimed at examining the actual response of the earth-filled embankment to external loads, a geodetic determination of displacements with the use of precise instruments is provided. The levelling measurements are most often performed due to their high accuracy and efficiency. An example of this is the study of the deformation of road embankment situated in permafrost region (Peng et al., 2015). Measurements of horizontal displacements are performed less frequently. However, they are applied to control the position and deformation of engineering structures such as bridges (Owerko et al., 2012) or retaining walls (Sukta and Kuras, 2013), hydrotechnical objects such as concrete dams (Yigit et al., 2016; Barzaghi et al., 2018) or tailings disposal facilities (Jamiolkowski, 2014), and special constructions such as telescopes (Niemiec et al., 2015). In some cases, they are determined also for earth-fill embankments. Guler et al. (2006) use the angular-linear network for this purpose and show the horizontal displacements of the 30-meter earth-filled dam between 2.8 and 40 mm over a period of five years. In addition, Tedd et al. (1994) describe the observation of horizontal movements of 9 mm in opposite directions due to the emptying and refilling the reservoir above the levee.

However, the horizontal displacements are the common quantity determined for gravity dams. For this type of objects research is carried out in order to point out the appropriate measurement methodology. It includes classic surveying observations and GNSS networks. Kalkan (2014) indicates that the differences in displacement values determined by these techniques are not greater than 10 mm, while the required measurement accuracy for horizontal displacement of rock-fill dams is 20–30 mm. A similar analysis was performed by Yavaşoğlu et al. (2018), giving detailed results for 30 points, for which the difference between classic and GNSS results equals ca. 8 mm (mean absolute error) for a period of 6 years. In both cases the displacements are significant, in the order of 3 cm/year. Similar values of differences between classic and GNSS measurements were obtained by Dardanelli and Pipitone (2017). They do not exceed 8 mm, however in this case the displacements are small and do not exceed the error values of their determination. Nevertheless, in a situation of small displacements a large number of observations is helpful. Based on them, reliable conclusions can be drawn, e.g. about the movement of the dam in the directions consistent with the occurring phenomenon – emptying and filling the reservoir (Pipitone et al., 2018).

## 2 Experimental flood embankment

In order to achieve the assumed goals, a temporary 4.5-metre experimental flood embankment was built on the terrace of the Vistula River, about 30 km from Kraków (Poland), consisting of two 180-metre parallel sections connected to each other in the form of a closed elongated ring (Fig. 1). The embankment formed a small reservoir that was filled periodically during the experiments in a way reflecting the passage of flood waves typical for the Upper Vistula basin. It had the form of a classic embankment (Tab. 1). All slopes were protected by a sod, and a temporary road made of hardened stone gravel was built on the embankment's crest.

Various soil materials were used for the construction of the embankment (marked in Fig. 2 with the following symbols: A, B, C, D, E) originating from adjacent areas. They are characterized by variable granulometric composition from medium sand/silty sand (MSa/siSa) to loam (saclSi) and different coef-

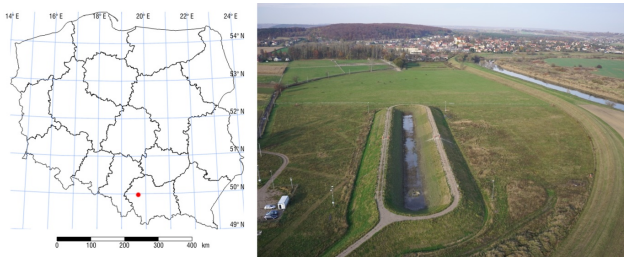


**Figure 1.** Experimental flood embankment – bird's-eye view (photo: S. Bazan)

**Table 1.** Geometrical parameters of the experimental embankment

Parameter	Actual (controlled) value
Height ( $H$ )	ca. 4.50 m
Elevation of the crest	216.10 m a.s.l.
Width of the crest	2.90–3.05 m
Slope of the western embankment	1:2 (downstream) 1:2 (upstream)
Slope of the eastern embankment	1:2 (downstream) 1:2.5 (upstream)

ficients of permeability from  $5.4 \cdot 10^{-7}$  to  $3.1 \cdot 10^{-5}$  m/s (Tab. 2), meeting the design guidelines, standards and requirements of the design team (Polish Committee for Standardization, 1997; Wolski et al., 1998).

Such variability allowed for a broader approach to monitoring and assessment of the behaviour of different materials under the same working conditions. To slightly diversify experimental research, in the northern part of the western embankment, drainage pipes imitating the presence of animals were built in (Fig. 2). Similarly, a silty sand lens was placed in the southern part. The presence of animals and burrows can be an indicator of damage to the embankment. When damming water, they constitute a preferential filtration route and contribute to the development of filtration and erosion processes inside the embankment. To limit the filtration through the subsoil, the bottom of the reservoir and the base of the levee's body were lined with a bentonite mat.

The degree of compaction  $I_S$  was adopted as the basic parameter for the quality control of embankments density. Its value ranged from 0.92 to 0.95. It fulfilled the compaction requirements (Polish Committee for Standardization, 1997) for the newly constructed embankments body of class III and IV for which  $I_S \geq I_{Sw}$  (0.92).

In order to observe the changes resulting from periodic accumulation of water in the reservoir (periodic external loads from accumulated water) or from dynamic loads (embankment thickening) which the levee was subjected to, continuous monitoring based on built-in measuring instruments (Fig. 3) and periodical surface monitoring were conducted. Monitoring inside the embankment included local measurements: pore pressure

**Table 2.** Material used for embankment construction

Material type*	Coefficient of permeability [m/s]	
	Range	Average
A siSa/saSi	$5.56 \cdot 10^{-7} \div 1.89 \cdot 10^{-5}$	$9.46 \cdot 10^{-6}$
B saSi/saSi	$(1.03 \div 8.62) \cdot 10^{-6}$	$3.44 \cdot 10^{-6}$
C MSa/siSa	$(3.04 \div 5.75) \cdot 10^{-5}$	$4.78 \cdot 10^{-5}$
D siSa/MSa	$(2.25 \div 4.15) \cdot 10^{-5}$	$3.08 \cdot 10^{-5}$
E saSi	$(5.26 \div 5.56) \cdot 10^{-7}$	$5.41 \cdot 10^{-7}$

\* according to ISO (2017a,b)

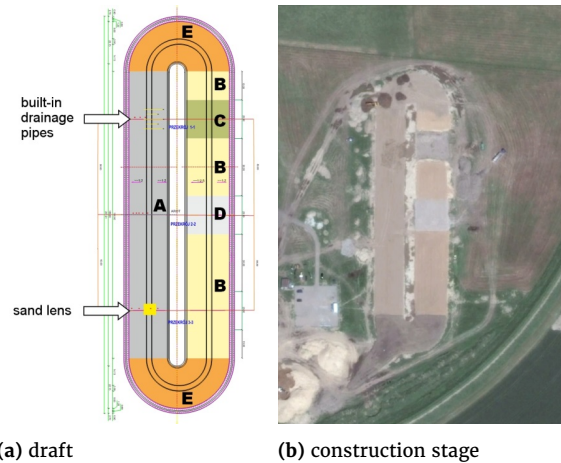


**Figure 2.** The distribution and type of material constituting the embankment (image source: Google Earth)

(35 items), total pressure (6 items) and moisture (20 items). Thermomonitoring based on quasi-linear (2D) measurements using fiber optic technology (ca. 1300 m of cable) were also carried out as well as point measurements which, if properly dense, allowed to obtain a quasi-spatial (3D) temperature distribution over time (Sekula et al., 2017). Additionally, 6 inclinometers (with a length of 6.5 m each) and 24 open piezometers (with a total length of 82 m) were installed in the embankment. A weather station was also located near the embankment to monitor local weather conditions. The measurements provided by the sensor network during experiments are the main element of the leakproofness assessment, and indirectly also the stability assessment of the embankment.

In addition, surface monitoring was carried out based on classical geodetic methods (leveling, tacheometry), ground-based radar interferometry (IBIS-L, IBIS-S) and geophysical monitoring using the electrical resistivity tomography (ERT) and ground penetrating radar (GPR). During the experiments, infrared cameras were also used (Stanisz et al., 2015).

### 3 Methodology for determining displacements

The structure subjected to observations as part of this work required a comprehensive development of the methodology for geodetic determining of displacements. A relatively small area of research made it possible to design an observation network allowing for high measurement accuracy. Moreover, it was necessary to design and establish the markers constituting the observation network, properly plan the measurements, and correctly perform them.

#### 3.1 Establishing the geodetic network

For the needs of research works conducted on the experimental embankment, an appropriate network of reference points and survey markers has been designed and established. The observation network was adapted to the planned geodetic observations using precise instruments: digital level, total station and the IBIS-L interferometric radar. Due to the type of conducted experiments, it was particularly important to determine displacements in the east-west direction, which is transversal to the reservoir axis. Based on previous numerical calculations, this is the direction of expected movements.

The basis of the network were reference points (Fig. 4),

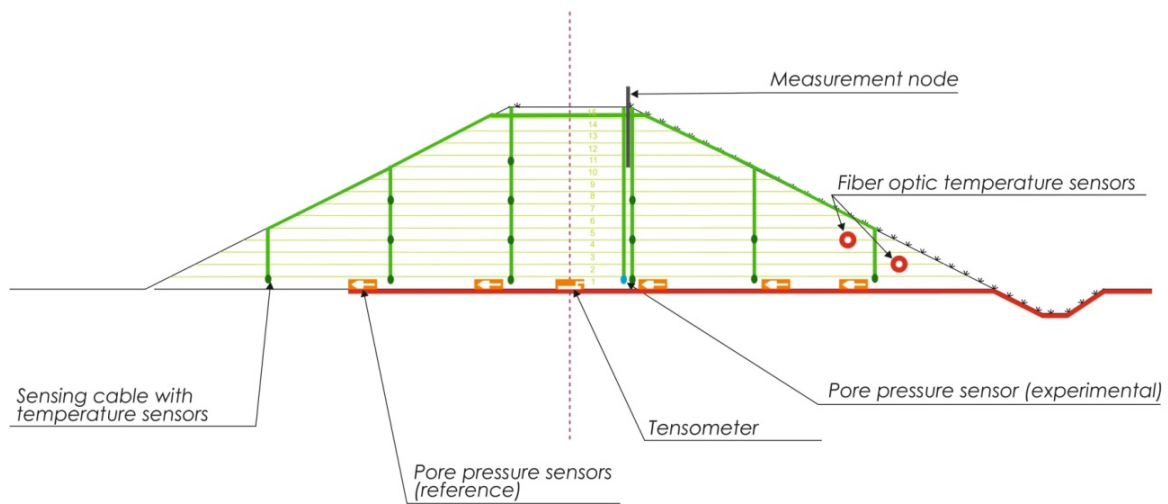


**Figure 3.** General location scheme of the sensors of experimental and reference measurement network placed in the experimental flood embankment (Sekula et al., 2017)



(a) design, dimensions in mm (b) reinforcement during construction (c) final application

**Figure 4.** Observation pillar constituting a reference point

which were designed as reinforced concrete pillars providing forced centering provided by a brass plate with a central screw. In addition, the benchmarks were installed on the pillars as reference points for height measurements, however the development of these measurements is not the subject of this publication. The aboveground part of the pillar was encased with a casing pipe, which was filled with thermally insulating material.

Three types of survey markers (Fig. 5) were designed and installed in the field:

- type 1 (14 pieces) – for radar, tachymetric and levelling observations,
- type 2 (18 pieces) – for tachymetric and levelling observations, established on the embankment slope,
- type 3 (16 pieces) – for tachymetric and levelling observations, established on the embankment crest.

All types of markers consist of a steel rod with a length of 1.5 m set in the ground, finished at the top with a concrete stub. The type 3 marker has a pin embedded in a concrete stub, which acts as a benchmark, with a hole constituting the center. Determining the position of these points required temporary

centering using a tripod and plummet. Permanent stabilization was impossible, because the technological road ran along the embankment crest. For type 1 and 2 markers, it was planned to embed a steel profile in the concrete stub, allowing for permanent installation of the benchmark and both prism and radar reflectors, which can be rotated in any direction without changing the center's position. Type 1 and 2 markers were installed on slopes and foreground of the embankment. Type 1 markers were installed on the western levee, which was observed with an interferometric radar, however the development of these measurements is not the subject of this publication.

### 3.2 Periodic measurements

The designed and finally established angular-linear observation network consists of 5 observation pillars and 48 survey markers (types 1, 2 and 3). The distribution of points is shown in Fig. 6. Each periodic measurement included ca. 130 directions and 130 distances. With the exception of two survey markers, partially obscured by terrain obstacles, the position of remaining 46 survey markers were determined by redundant measurements. The surveying was performed with a robotic

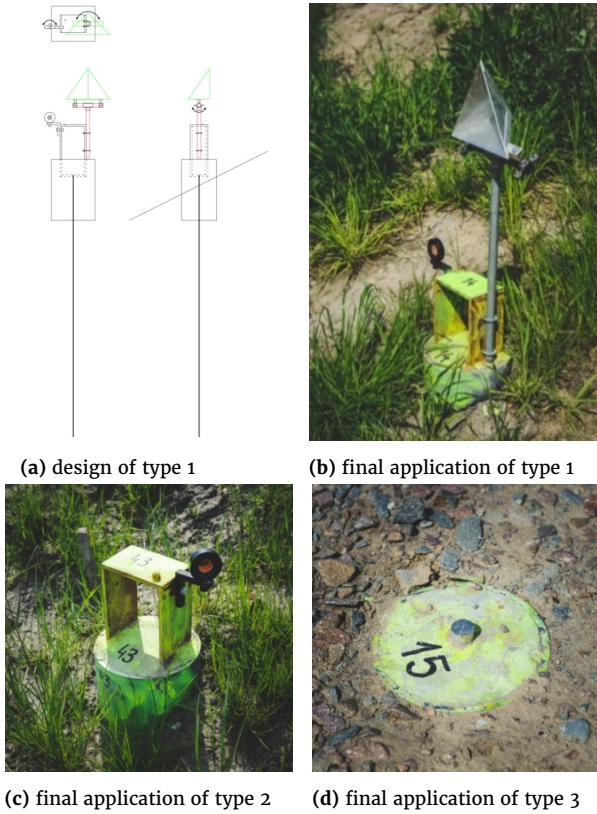


Figure 5. Design and final application of observation markers on the structure

instrument in several sets, in an automatic way, with the errors  $\sigma_{angle} = 1''$  and  $\sigma_{dist} = 1,5 \text{ mm} + 1 \text{ ppm}$ . Additive constant values for all prism reflectors had been previously determined. Before the measurement, the instrument was adapted to the current atmospheric conditions. Considering the number of unknowns, the network has ca. 140 redundant observations.

Five reference points together with four fixed markers formed the network for determining the reference frame for the studied structure. The stability of the reference points was checked on the basis of a 4-parameter conformal transformation between the original coordinate system, in which the coordinates of points from the previous epoch were expressed  $(x_{oi}, y_{oi})$ , and the current coordinate system used for the current coordinates expression  $(x'_{oi}, y'_{oi})$ . Transformation parameters are denoted as:  $\Delta x$ ,  $\Delta y$  – translations along the  $x$  and  $y$  axes,  $\varphi$  – rotation between coordinate systems,  $s$  – scale factor.

Transformation parameters were determined based on the redundant system of equations created for all potential reference points, using the least squares method:

$$\begin{cases} x_{oi} = \Delta x + bx'_i - ay'_i \\ y_{oi} = \Delta y + ax'_i + by'_i \end{cases} \quad i = 1, \dots, 5, \quad (1)$$

where:

$$\varphi = \arctan\left(\frac{a}{b}\right), \quad (2)$$

$$s = \sqrt{a^2 + b^2}. \quad (3)$$

The horizontal displacements of points ( $d_{xy}$ ) were calculated based on the adjusted transformation parameters ( $\Delta\hat{x}$ ,  $\Delta\hat{y}$ ,  $\hat{\varphi}$ ,  $\hat{s}$ ) as the difference between the current coordinates transformed into the original coordinate system and the coordinates from

Table 3. Adjustment errors for long-term monitoring observations

Error	Dec15	Nov16	Apr17
$\hat{\sigma}_{posit2D,max}$	1.6 mm	1.2 mm	0.9 mm
$\hat{\sigma}_{posit2D,rms}$	1.1 mm	0.8 mm	0.6 mm
$\hat{\sigma}_{dist,max}$	1.1 mm	0.8 mm	0.6 mm
$\hat{\sigma}_{dist,rms}$	0.5 mm	0.4 mm	0.3 mm
$\hat{\sigma}_{dir,max}$	0.34 mgon	0.26 mgon	0.19 mgon
$\hat{\sigma}_{dir,rms}$	0.27 mgon	0.19 mgon	0.17 mgon

the original measurement:

$$\begin{cases} dx_i = x_i - x_{oi} = \Delta\hat{x} + \hat{b}x'_i - \hat{a}y'_i - x_{oi}, \\ dy_i = y_i - y_{oi} = \Delta\hat{y} + \hat{a}x'_i + \hat{b}y'_i - y_{oi}, \end{cases} \quad (4)$$

$$d_{xy,i} = \sqrt{dx_i^2 + dy_i^2}, \quad (5)$$

where:  $x_i$ ,  $y_i$  – coordinates from the current measurement transformed into the original coordinate system.

If the  $d_{xy}$  value exceeded twice the error of its determination, the point was rejected from the group of reference points. As further results show, this situation did not occur in the presented research. Finally, the displacements of all 48 survey markers were also calculated according to Eqs. (4–5).

## 4 Results of displacement observation

Geodetic measurements were carried out for two purposes. The first was long-term monitoring, which was aimed to determine the influence of atmospheric factors (e.g. soil freezing), vehicles moving on the embankment body or vestigial subsidence of the newly built embankment. The second purpose was to check the behaviour of the embankment as a result of filling and draining the reservoir.

### 4.1 Long-term displacement monitoring

Long-term observations included three measurements taken in December 2015, November 2016 and April 2017. Accuracy of measurements is presented in Tab. 3, which contains the maximum and root mean square errors of: horizontal position ( $\hat{\sigma}_{posit2D}$ ), distance ( $\hat{\sigma}_{dist}$ ) and direction ( $\hat{\sigma}_{dir}$ ).

In the course of calculations, it was found that all reference points remained stable (Tab. 4). Their residual displacements  $d_{xy}$  did not exceed 0.8 mm, while the error of determining these values ( $\sigma_{dxy}$ ) was not less than 1.0 mm. The mean error of mutual fitting of reference points ( $\sigma_{transform}$ ) did not exceed 0.4 mm. The determined transformation parameters were used to calculate the displacements of all network points. Their values are presented in Tab. 5.

Fig. 7 shows the displacement values for both long-term intervals: 2015–2016 and 2016–2017. The results clearly indicate the dominance of displacements outside the reservoir for points located on the embankment. Points on the crest do not show significant movements (visible vectors may result from centering errors), like those on the foreground (except one, north-west point, which had been defectively established in the field).

After determining the dominant movements in the E-W direction for points located on the eastern and western embankments, the average displacement values were calculated for groups of points located at the same height. Only the E-W component of the displacement was used for the calculation. The results are summarized in Tab. 6 and presented in

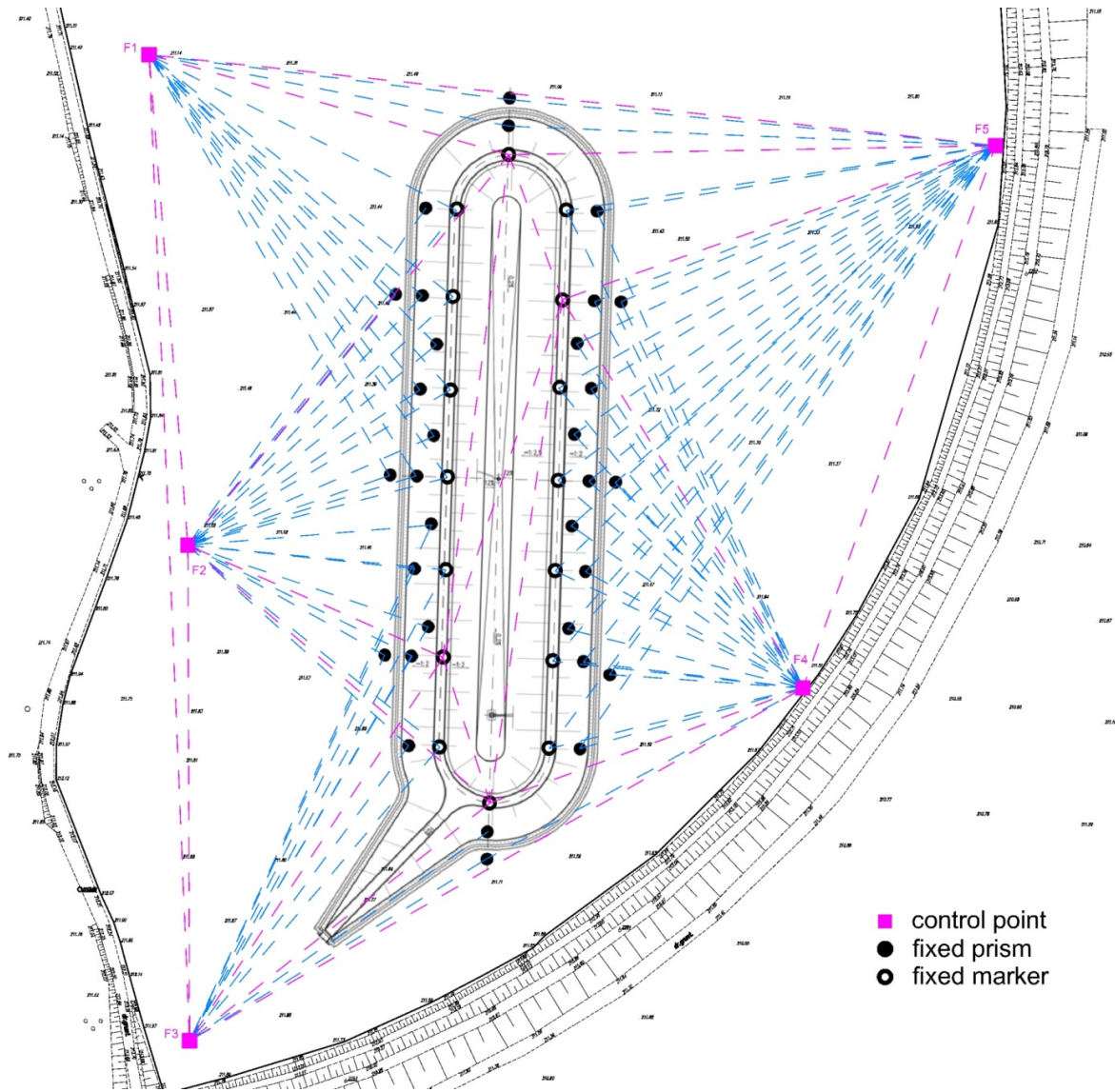


Figure 6. Observations in control network (violet lines – measurements between reference points, blue lines – measurements to the survey markers)

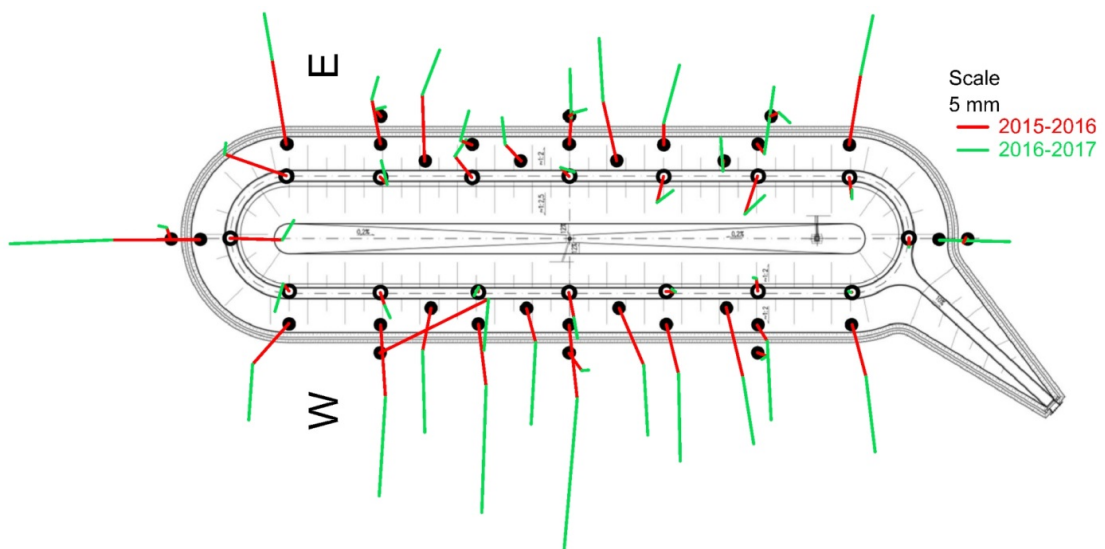


Figure 7. Long-term displacements

**Table 4.** The residual displacements of reference points with their errors (all values in mm)

Point	Dec15 – Nov16		Nov16 – Apr17		
	$d_{xy}$	$\sigma_{dxy}$	$d_{xy}$	$\sigma_{dxy}$	
	$d_{xy}$	$\sigma_{dxy}$	$d_{xy}$	$\sigma_{dxy}$	
F1	0.39	1.4	0.39	1.0	
F2	0.73	1.4	0.56	1.0	
F3	0.43	1.4	0.52	1.0	
F4	0.73	1.4	0.58	1.0	
F5	0.40	1.3	0.25	1.0	
		$\sigma_{transform} = 0.39$		$\sigma_{transform} = 0.34$	

**Table 5.** The transformation parameters between previous and current epoch

Parameter	Dec15 – Nov16	Nov16 – Apr17
$\Delta\hat{x}$ [mm]	-0.22	-1.08
$\Delta\hat{y}$ [mm]	0.22	0.58
$\hat{\phi}$ [mgon]	0.102	-0.053
$\hat{s}$ [-]	1.00000031	1.00000976

Fig. 8. Mean values and their standard deviations are denoted as  $d_{15-16} \pm \sigma_{d_{15-16}}$  and  $d_{16-17} \pm \sigma_{d_{16-17}}$ .

The cause of the displacement may be the influence of atmospheric factors (e.g. soil freezing), vehicles moving on the embankment body or vestigial subsidence of the newly built embankment. Another explanation may be the frost heave of the soils used for the construction of the embankments causing swelling effect particularly in their upper part. In addition, points located on the western embankment show approx. 1.7 times larger displacements than on the eastern side, which may result from the diversification of soils forming the two embankments.

Average values and the standard deviations confirm the small movement of points located on the crest and on the foreground. For points located on the slopes, the western side has a clearer tendency of movement of the whole group (smaller standard deviations). The reason may be the lack of diversity in the construction of individual sections of the embankment that was present on the eastern side.

#### 4.2 Filling and draining experiment

During conducting a series of tests on flood embankment, the influence of the increase (Fig. 9) and decrease of the water level on the levee's behaviour was checked. As a result of numeri-

**Table 6.** Average long-term E-W displacements and their standard deviations (all non-integer values in mm)

Group of points	Embankment W			Embankment E		
	No. of pts	$d_{15-16}$	$\sigma_{d_{15-16}}$	No. of pts	$d_{15-16}$	$\sigma_{d_{15-16}}$
		$d_{16-17}$	$\sigma_{d_{16-17}}$		$d_{16-17}$	$\sigma_{d_{16-17}}$
Crest	7	-0.3	2.2	7	-0.9	4.1
		-1.5	2.0		2.0	1.5
2/3 of H (3.0 m)	4	-8.7	2.7	4	5.7	6.2
		-12.7	1.3		7.0	2.6
1/3 of H (1.5 m)	7	-8.9	3.4	7	5.9	5.8
		-16.3	5.5		7.9	2.7
Foreground	2	-1.8	1.6	3	0.8	0.4
		-0.2	0.4		-0.3	1.3

**Table 7.** Average E-W displacements determined during reservoir filling (all values in mm)

Group of points	Embankment W					$\Sigma$
	int.1	int.2	int.3	int.4	int.5	
Crest	-1.0	1.0	-0.6	-0.5	0.8	-0.2
2/3 of H (3.0 m)	-1.7	-0.1	-0.4	0.0	3.1	0.9
1/3 of H (1.5 m)	-0.9	-0.3	-0.1	-0.8	2.5	0.4
Foreground	-0.5	-0.4	-0.5	0.4	-0.3	-1.3
Embankment E						
Crest	1.3	-1.8	0.7	0.4	-0.7	-0.1
2/3 of H (3.0 m)	1.3	-0.3	0.5	-0.1	-1.8	-0.4
1/3 of H (1.5 m)	0.9	-0.1	0.2	0.1	-0.8	0.3
Foreground	1.2	-0.3	-0.4	0.0	0.8	1.4

cal analyses, horizontal displacements were obtained (Fig. 10). In calculations a continuous increase of water level up to 4 m during 96 hours and decrease within 120 hours were assumed (Stanisz et al., 2017).

The numerical simulations were made in plane state of strain with the use of FLAC 2D v. 7.0. The simulation did not take into account the filter-erosion deformation associated with seepage in the levee. It was carried out for levees built of homogeneous cohesive materials with different filtration coefficients. In calculations an elastic-plastic mechanical model with use of Mohr-Coulomb strength criterion was assumed. The model was discretised with a regular grid of 0.25 m for the levee and 0.5–1.0 m for lower layers. A more detailed description of the numerical simulation is presented by Stanisz et al. (2017).

It should be emphasised that the short time of increase and decrease of the water level limited the development of deformation in the levee. Under the conditions of the field experiment, the asymmetric levee built of silty sand was more susceptible to deformation, with higher pore pressure values (Stanisz et al., 2017).

The course of the experiment simulating the flood wave is shown in Fig. 11. The periods of filling up and draining the reservoir are marked, as well as the water level. The "X" symbol indicates the days when the geodetic angular-linear network was measured in order to determine displacements of the embankment.

The method of determining displacements was analogous to the long-term monitoring, thanks to which the obtained measurement accuracy was equally high. The reference points F1–F5 invariably remained stable and served as the reference base for determining displacements of the remaining points. The results of displacement determination for all five time intervals are presented in Fig. 12.

Due to the low values of displacements, often at the level of their determination errors, the graph seems to be quite illegible. For this reason, only the E-W components of displacements were selected for further calculations, as they were expected in numerical analyses. In addition, points were divided into groups according to the height of their foundation, as in Chapter 4.1. Averaging the values of displacements (Tab. 7) allows to perceive some tendencies (Fig. 13).

In the interval 1 the reservoir was filled with water and the embankment was soaking for a few days. All observed points then showed movement outside of the reservoir by an average of 1.2 mm. Then, in the interval 2, when the reservoir was emptied, the opposite tendency of points located on the crest was visible. The remaining points did not show significant (more than 0.5 mm) changes in location. In short intervals 3 and 4, when the reservoir was filled twice, the displacement val-

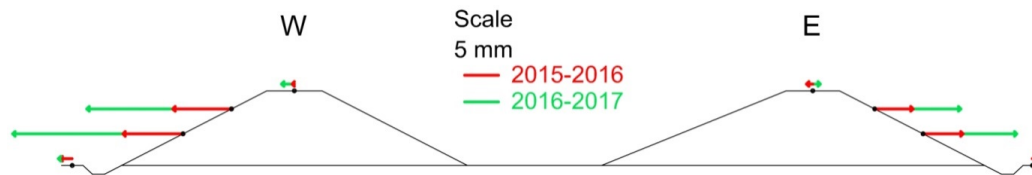


Figure 8. Average long-term E-W displacements for groups of points situated at the same height



Figure 9. The reservoir filled with water – bird's-eye view (photo: S. Bazan)

ues are small (0.3 mm on average), although there is a tendency of movement outside the reservoir for points located on the embankment. Finally, in a relatively long interval 5, when the levee could dry up, the points located on the embankment clearly moved inside of the reservoir (1.6 mm on average), returning more or less to their position before the filling experiments had started. It is illustrated by the values marked as  $\Sigma$  in Tab. 7, which are smaller than 0.5 mm in most cases. This return tendency is not shown by points on the foreground, for which a 1.0–1.5 mm displacement outside the reservoir can be found.

On the basis of the above analysis, the relation between water reservoir soaking and the directions of embankment movement can be noticed. During periods of filling the reservoir and for some time after its draining, when the levee was still saturated with water, movements outside the reservoir were revealed. On the other hand, the following long period of drying caused movement in the opposite direction.

This behaviour is characteristic for earth-filled structures like flood embankments, which are practically unsaturated most of the time. During the freshets as a result of changes in the moisture of the embankment body, a phenomenon of swelling is observed. As a result of dampness, the suction force decreases, thereby lowering the pressure at the contact points of the soil particles. The water films then strive to fully fill the voids by adsorptive suction of water molecules. As a result, water is sucked into the pores. The water content in the ground increases and the suction pressure decreases. Particles of the soil are moving away from each other causing a swelling effect (Grabowska-Olszewska, 1998).

As a result of lowering the water in the reservoir and thus lowering the filtration curve in the embankment body, the opposite effect is obtained. Then, negative water pressures in the pores of the ground (passive capillarity) occurring above the lowering water table cause the increase of soil effective stresses and the capillary menisci retreat deeper into the narrowing pores. As a result, an increasing underpressure occurs, and thus the increasing stress in the ground skeleton (effective stress). In this way, the volume of the soil is reduced, which means shrinkage. This is due to the fact that with rising suction pressure the air enters the pores, and the compressible membrane begins to form around the contact points between the soil particles (Grabowska-Olszewska, 1998).

## 5 Conclusions

The results of geodetic measurements allow to indicate the reaction of embankment to external loads. In the case of long-term monitoring, the movement may be caused by atmospheric factors (e.g. soil freezing), vehicles moving on the embankment body or vestigial subsidence of the newly built embankment, and also by the frost heave of the soils used for the construction of the embankments. On the other hand, in the case of flood wave simulation, the relation between water reservoir soaking and the directions of embankment movement can be noticed. Horizontal displacements indicate that in some cases earth-filled structures may behave to some extent like elastic structures. The movement occurs in the horizontal direction generally in accordance with the change in the horizontal component of the water pressure depending on the water level in the reservoir.

However, it should be noticed that the determined displacement values are often not much greater than the errors of their determination. This may be the reason for some non-compliances with numerical calculations. Nevertheless, thanks to the large number of points established on the embankment, it is possible to determine the existence of some trends that may be related to the conducted experiments.

Changes in soil moisture in the aeration zone can occur within strictly defined limits, from extremely dry to fully saturated. Based on the shape and course of the curve characterizing the ground-water system, a number of information on the potential possibility of a given ground to absorb or lose water can be obtained. With information on the current humidity or saturation of the tested soil, the shrinkage or swelling of the soil may be concluded, and thus prediction of deformation processes.

In further work, it is planned to compare the results of geodetic measurements with the values of horizontal displacements recorded by the ground-based interferometric radar operating in continuous mode during filling and draining the reservoir. The aim of the work will be to assess the compliance of both methods and indicate their limitations in observations of earth-filled structures. An important stage of further research will also be an attempt to determine the causes of the detected long-term movements. For this purpose, various measurements (i.a. precise levelling and built-in sensor records) will be used.

## Acknowledgements

The research presented in this paper was supported by National Centre for Research and Development (NCBiR) under the grant No. PBS1/B9/18/2013. The geodetic analyses were carried out by AGH University of Science and Technology, Department of Engineering Surveying and Civil Engineering, as a part of statutory project No. 11.11.150.005. Currently, the geotechnical analyses are carried out by AGH University of Science and Technology, Department of Hydrogeology and Engineering Geology, as a part of statutory project No. 11.11.140.649.

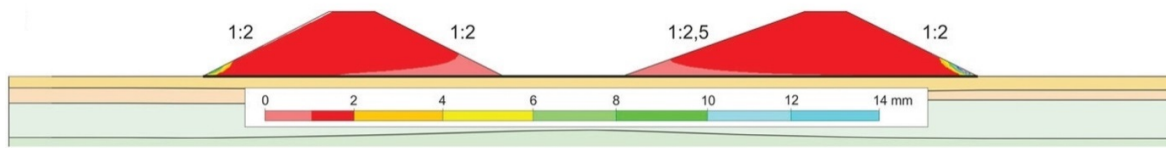


Figure 10. Numerical simulation of horizontal displacement inside the levee for an increase in water level to a height of 4 m (Stanisz et al., 2017)

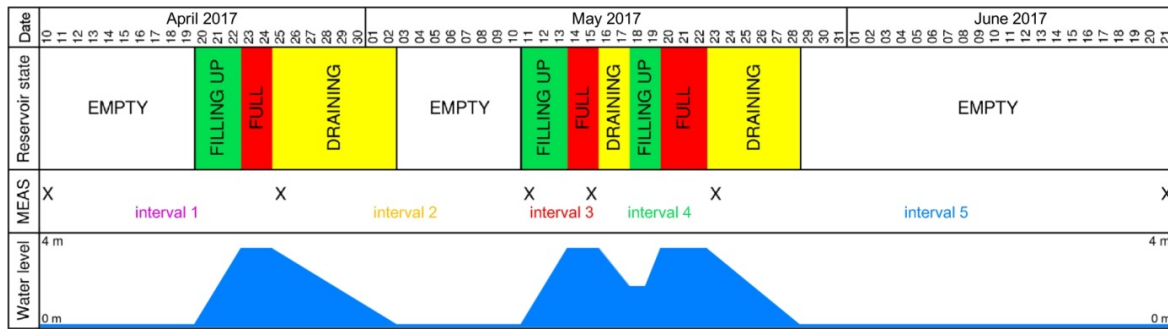


Figure 11. The course of the experiment with the marking of surveying measurements days



Figure 12. Displacements determined during reservoir filling

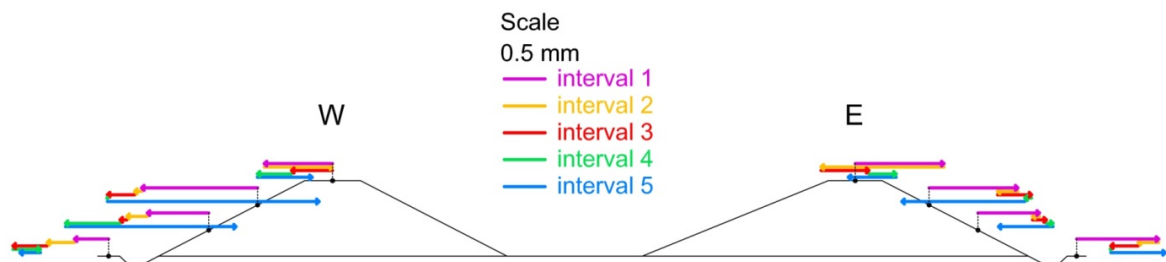


Figure 13. Average E-W displacements determined during reservoir filling for groups of points situated at the same height

## References

- Barzaghi, R., Cazzaniga, N. E., De Gaetani, C. I., Pinto, L., and Tornatore, V. (2018). Estimating and comparing dam deformation using classical and GNSS techniques. *Sensors*, 18(3):756, doi:10.3390/s18030756.
- Borecka, A. (2016). Monitoring wałów przeciwpowodziowych w systemie bezpieczeństwa powodziowego. *Geoinżynieria: drogi, mosty, tunele*, 57(4):40–44.
- Dardanelli, G. and Pipitone, C. (2017). Hydraulic models and finite elements for monitoring of an earth dam, by using GNSS techniques. *Periodica Polytechnica Civil Engineering*, 61(3):421–433, doi:10.3311/PPci.8217.
- Filaber, J., Kosowski, B., and Borecka, A. (2016). *Ochrona przeciwpowodziowa w systemie zarządzania kryzysowego*. Texter Sp. z oo.
- Ghorbani, M., Sharifzadeh, M., Yasrobi, S., and Daiyan, M. (2012). Geotechnical, structural and geodetic measurements for conventional tunnelling hazards in urban areas – the case of Niayesh road tunnel project. *Tunnelling and Underground Space Technology*, 31:1–8, doi:10.1016/j.tust.2012.02.009.
- Grabowska-Olszewska, B. (1998). *Geologia stosowana: właściwości gruntów nienasyconych*. Wydawnictwo Naukowe PWN.
- Guler, G., Kilic, H., Hosbas, G., and Ozaydin, K. (2006). Evaluation of the movements of the dam embankments by means of geodetic and geotechnical methods. *Journal of Surveying Engineering*, 132(1):31–39, doi:10.1061/(ASCE)0733-9453(2006)132:1(31).
- Hwang, C., Hung, W.-C., and Liu, C.-H. (2008). Results of geodetic and geotechnical monitoring of subsidence for Taiwan High Speed Rail operation. *Natural Hazards*, 47(1):1–16, doi:10.1007/s11069-007-9211-5.
- ISO (2015). *Geotechnical investigation and testing – Geotechnical monitoring by field instrumentation – Part 1: General rules*. (ISO Standard No. 18674-1).
- ISO (2017a). *Geotechnical investigation and testing – Identification and classification of soil – Part 1: Identification and description*. (ISO Standard No. 14688-1).
- ISO (2017b). *Geotechnical investigation and testing – Identification and classification of soil – Part 2: Principles for a classification*. (ISO Standard No. 14688-2).
- Jamiolkowski, M. (2014). Soil mechanics and the observational method: challenges at the Zelazny Most copper tailings disposal facility. *Géotechnique*, 64(8):590–618, doi:10.1680/geot.14.RL.002.
- Kalkan, Y. (2014). Geodetic deformation monitoring of Ataturk Dam in Turkey. *Arabian Journal of Geosciences*, 7(1):397–405, doi:10.1007/s12517-012-0765-5.
- Niemiec, J., Bilnik, W., Błocki, J., Bogacz, L., Borkowski, J., Bulik, T., Cadoux, F., Christov, A., Curyło, M., della Volpe, D., et al. (2015). Prototype of the SST-1M telescope structure for the Cherenkov Telescope Array. In *Proceedings of the 34th International Cosmic Ray Conference (ICRC2015), The Hague, The Netherlands.*, (arXiv:1509.01824).
- Owerko, T., Ortyl, ., Kocierz, R., Kuras, P., and Salamak, M. (2012). Investigation of displacements of road bridges under test loads using radar interferometry – case study. In *Proceedings of the 6th International Conference Bridge maintenance, safety, management, resilience and sustainability, Stresa, Italy*, pages 181–188.
- Peng, H., Ma, W., Mu, Y.-h., and Jin, L. (2015). Impact of permafrost degradation on embankment deformation of Qinghai-Tibet Highway in permafrost regions. *Journal of Central South University*, 22(3):1079–1086, doi:10.1007/s11771-015-2619-2.
- Pipitone, C., Maltese, A., Dardanelli, G., Lo Brutto, M., and La Loggia, G. (2018). Monitoring water surface and level of a reservoir using different remote sensing approaches and comparison with dam displacements evaluated via GNSS. *Remote Sensing*, 10(1):71, doi:10.3390/rs10010071.
- Polish Committee for Standardization (1997). *Urządzenia wodno-melioracyjne – Nasypy – Wymagania i badania przy odbiorze*. (PKN Standard No. PN-B-12095).
- Sekuła, K., Borecka, A., Kessler, D., and Majerski, P. (2017). Smart levee in Poland. Full-scale monitoring experimental study of levees by different methods. *Computer Science*, 18:357–384, doi:10.7494/cs.2017.18.4.2220.
- Stanisz, J., Borecka, A., Pilecki, Z., and Kaczmarczyk, R. (2017). Numerical simulation of pore pressure changes in levee under flood conditions. In *E3S Web of Conferences*, volume 24, page 03002. EDP Sciences. doi:10.1051/e3sconf/20172403002.
- Stanisz, J., Korzec, K., and Borecka, A. (2015). ISMOP project (IT system of levee monitoring) as an example of integrated monitoring of levee. *Geology, Geophysics and Environment*, 41(1):137–139, doi:10.7494/geol.2015.41.1.137.
- Sukta, O. and Kuras, P. (2013). A preliminary analysis of the use of non-invasive measurement methods in the studying the geometry of retaining walls. In *Proceedings of 13th International Multidisciplinary Scientific GeoConference SGEM2013*, volume 2, pages 17–24. STEF92 Technology. doi:10.5593/SGEM2013/BB2.V2/S09.003.
- Tedd, P., Charles, J., Holton, R., and Robertshaw, A. (1994). Deformation of embankment dams due to changes in reservoir level. In *Proceedings of XIII International Conference on Soil Mechanics and Foundation Engineering*, volume 3, pages 951–951.
- Wolski, W., Mirecki, J., and Mosiej, K. (1998). *Warunki techniczne wykonania i odbioru robót ziemnych*. Warszawa: Ministerstwo Ochrony Środowiska, Zasobów Naturalnych i Leśnictwa.
- Yavaşoğlu, H. H., Kalkan, Y., Tiryakioğlu, İ., Yigit, C. O., Özbey, V., Alkan, M. N., Bilgi, S., and Alkan, R. M. (2018). Monitoring the deformation and strain analysis on the Ataturk Dam, Turkey. *Geomatics, Natural Hazards and Risk*, 9(1):94–107, doi:10.1080/19475705.2017.1411400.
- Yigit, C. O., Alcay, S., and Ceylan, A. (2016). Displacement response of a concrete arch dam to seasonal temperature fluctuations and reservoir level rise during the first filling period: evidence from geodetic data. *Geomatics, Natural Hazards and Risk*, 7(4):1489–1505, doi:10.1080/19475705.2015.1047902.